November 2019. Horticultural Plant Journal, 5 (6): 255–267.

Horticultural Plant Journal

Available online at www.sciencedirect.com
The journal's homepage: http://www.keaipublishing.com/en/journals/horticultural-plant-journal

Comprehensive Characterization of miRNA and *PHAS* Loci in the Diploid Strawberry (*Fragaria vesca*) Genome

Lei Feng[a,b,c], *Rui Xia*[a,b,c,*], *and Yuanlong Liu*[a,b,c,*]

[a] *State Key Laboratory for Conservation and Utilization of Subtropical Agro-Bioresources, South China Agricultural University, Guangzhou 510642, China*

[b] *Key Laboratory of Biology and Germplasm Enhancement of Horticultural Crops in South China, Ministry of Agriculture, South China Agricultural University, Guangzhou 510642, China*

[c] *Guangdong Litchi Engineering Research Center, College of Horticulture, South China Agricultural University, Guangzhou 510642, China*

Received 7 August 2019; Received in revised form 8 October 2019; Accepted 27 October 2019

Available online 27 November 2019

A B S T R A C T

Small RNAs (sRNAs) are vital regulators of gene expression and involved in various biological processes. Among them, microRNAs (miRNAs) and phased small interfering RNAs (phasiRNAs) have been well defined and studied in the past decades. A bunch of scripts or pipelines were developed to annotate miRNAs and phasiRNAs. However, some computational annotations are rough and without careful manual check, resulting in low quality annotation. In this study, 19 public strawberry (*Fragaria vesca*) sRNA sequencing data from nine different tissues were collected to annotate miRNAs and *PHAS* loci in *F. vesca*. After bioinformatics analysis and careful manual checking, 167 known miRNAs, 27 miRNA*s with notable abundance, 54 novel miRNAs were accurately annotated. The terms of two miRNAs were corrected from miR477b and miR5225 using miRN47 and miR3627h, respectively. Besides 21 nucleotides (nt) miR390, eleven miRNAs with a length of 22-nt are in charge of triggering the biogenesis of 21-nt phasiRNAs from 110 *PHAS* loci in strawberry. In particular, we found several *PHAS* loci were targeted by two different miRNAs (similar to the "two-hit" model) and the phasiRNA generating region located between two target sites. We speculate that one target site is in control of triggering phasiRNA biogenesis and the other target site define the boundary of the region of phasiRNA biogenesis, which likely provide an accurate way for phasiRNA generation. Overall, we provided a comprehensive and accurate annotation of miRNAs and *PHAS* loci in the *F. vesca* genome.

Keywords: *Fragaria vesca*; miRNA; *PHAS* loci; annotation; phasiRNA biogenesis model

1. Introduction

In plants, small RNAs play essential roles in many aspects of biological processes (Bartel, 2004; D'Ario et al., 2017; Chen et al., 2018b). Based on the biogenesis and function, small RNAs were classified into different categories (Axtell, 2013). miRNA, which is typically 20- to 22-nt in length, is generated from a *MIR* transcript that harbors a hairpin structure. The *MIR* precursor is typically processed into miRNA/miRNA* duplex by DCL1, a Dicer-like protein, via accurate sequential slicing. The mature miRNA and miRNA* are released by helicase. Mature miRNA is thereafter methylated by HEN1 and incorporated into AGONAUTE1 (AGO1) to form an RNA-induced silencing complex (RISC) that regulates target genes by complementary nucleotide base-pairing (Li et al., 2005; Yu et al., 2005; Achkar et al., 2016). miRNA* is often considered as nonfunctional byproducts, because it will be degraded quickly and is much less abundant than its corresponding mature miRNA. However, a previous study showed that miR393* was enriched in AGO2, suggesting that miRNA* may be biologically functional (Zhang et al., 2011). Typically,

* Corresponding. Tel.: +86 20 38348652
E-mail addresses: rxia@scau.edu.cn; liuyuanlong@scau.edu.cn

Peer review under responsibility of Chinese Society for Horticultural Science (CSHS) and Institute of Vegetables and Flowers (IVF), Chinese Academy of Agricultural Sciences (CAAS)

https://doi.org/10.1016/j.hpj.2019.11.004

a canonical miRNA, which is 21-nt in length, represses target genes by directly slicing or translation repression (Voinnet, 2009). In some cases, when an asymmetric bulge occurs on the miRNA strand within the duplex, it will generate a 22-nt miRNA and a 21-nt miRNA* by DCL1. The 22-nt miRNA loaded into AGO1 could not only slice its target genes but also trigger the biogenesis of phasiRNAs (Chen et al., 2010; Cuperus et al., 2010). After 22-nt miRNA-mediated slicing, RNA-dependent RNA polymerase 6 (RDR6) is recruited to convert the 3′ cleaved fragment into double-strand RNA (dsRNA). Later on, the dsRNA is processed by DCL4 / DCL5 into 21-/24-nt phasiRNAs respectively starting from the cleavage site (Fei et al., 2013). The mechanism of 22-nt miRNA-directed phasiRNA biogenesis is termed as "one-hit" model. Another mechanism for phasiRNA biogenesis is the 21-nt miR390-mediated "two-hit" model. miR390 bound to AGO7 targets *TAS3* through two target sites. The 5′ proximal target site is always non-cleavable while 3′ proximal target site is cleavable. After cleavage, 5′ fragment of *TAS3* is selected as a substrate for producing phasiRNAs (Axtell et al., 2006; Montgomery et al., 2008; Fei et al., 2013).

To date, a lot of studies have indicated that miRNAs and phasiRNAs are involved in different biological processes, such as plant development (Wu et al., 2006; Marin et al., 2010; Cho et al., 2012; Guan et al., 2014; Lin et al., 2015; Hobecker et al., 2017; Liu et al., 2017b; Guo et al., 2018), defense responses (Si-Ammour et al., 2011; Liu et al., 2014; Cui et al., 2015; Fei et al., 2016; Cai et al., 2018; Wang et al., 2018; Hou et al., 2019) and abiotic stress resistance (Li et al., 2014, 2016; Shuai et al., 2016; Liu et al., 2017a; Sosa-Valencia et al., 2017; Xie et al., 2017) etc. Since miRNAs and phasiRNAs act as vital regulators, a few researches have been done on strawberry miRNAs. At the very beginning, microarray and computational identification based on homology were used to identify miRNA in strawberry (Li et al., 2009b; Dong et al., 2012). With the development of high-throughput sequencing technology and the release of strawberry genome (Shulaev et al., 2011), sRNA sequencing was widely used to characterize miRNAs (Ge et al., 2013; Li et al., 2013; Xu et al., 2013; Xia et al., 2015b, 2019; Šurbanovski et al., 2016; Liang et al., 2018) as well as phasiRNAs (Xia et al., 2015b, 2019) while degradome sequencing was used to identify the target genes for them (Xia et al., 2015b; Šurbanovski et al., 2016; Li et al., 2019). To efficiently tackle the vast amount of sequencing data, lots of pipelines were developed. However, some computational analyses are not accurate enough, leading to improper annotation, such as fve-miR5225 and fve-miR1030, which should be grouped into miR3627 and miR530 family, respectively. Moreover, inaccurate computational annotations may also result in incorrect registration in miRbase, for example, the fve-miR477b in miRbase shows no sequence similarity to other miR477 members. Meanwhile, the term of some strawberry miRNA is disordered, for example, miR164f in *Fragaria* × *ananassa* was assigned based on the similarity to osa-miR164f rather than the number of loci in *Fragaria* × *ananassa* genome (Han et al., 2014). Previous studies on strawberry miRNAs focused on a certain or few tissues, leading to incomplete miRNA / *PHAS* loci identification (Šurbanovski et al., 2016; Xia et al., 2015b, 2019). Analyzing large-scale biological datasets may improve the accuracy of authentic miRNA identification (Axtell and Meyers, 2018). Thus, we collected 19 sRNAs sequencing data from 9 different tissues of *F. vesca* and annotated miRNAs by in-house software sRNAminer, manually checking each accession following the criteria updated recently (Axtell and Meyers, 2018) in order to provide accrate and comprehensive miRNA annotation for strawberry. We also annotated all miRNAs and miR2275 in strawberry genome. Furthermore, four degradome data were used to genome-widely profile the regulatory pathway directed by miRNAs and related phasiRNAs.

2. Materials and methods

2.1. Collection of strawberry sRNA and degradome sequencing dataset

Nineteen sRNA sequencing data and 4 degradome sequencing data from diploid strawberry (*F. vesca*) were downloaded from NCBI (Table 1). Three sRNA sequencing data of strawberry flower were collected from GEO accession number GSE44930 (Xia et al., 2013). From accession number GSE61798, we downloaded eight sRNA sequencing data including four different tissues and three degradome data from mixed tissues (Xia et al., 2015b). We got four sRNA sequencing data and one degradome data via accession number PRJNA282518 (Šurbanovski et al., 2016). sRNA sequencing data from four development stages of anther were downloaded with the accession number SRP149613 (Xia et al., 2019). Detailed information was supplied in Table 1.

2.2. Data preprocessing

Fasterq-dump was used to convert the original data from sra format to fastq format (https://github.com/ncbi/sra-tools/wiki/HowTo:-fasterq-dump). Dnapi.py was then used to predict the adaptor of sRNA sequencing data (https://github.com/jnktsj/DNApi). After that, we used an in-house software 'sRNAminer' to do a series of preprocessing for sRNA sequencing data. First, sRNAseqAdaperRemover from sRNAminer was utilized to remove the adaptor of sRNA sequencing data based on previously predicted adaptor and remove short reads, whose length was less than 15. Then, sRNAseqCollasper was used to collapse reads of the same sequence. After that, the clean reads were aligned to Rfam and The Plant Organelles Database to remove noncoding RNAs (rRNA, snoRNA, and tRNA) and DNA from chloroplast and mitochondrial genomes by bowtie allowing one mismatch within the alignment (Langmead, 2010; Mano et al., 2014; Kalvari et al., 2018). The same bowtie parameter was applied to map clean reads to the *F. vesca* V4.0 genome. sRNAseqAlignmentFormater and sRnaAlnIndexBuilder were subsequently used to convert the format of bowtie files and sort the file based on the position of reads mapped on the genome, respectively.

2.3. miRNA identification

In order to get high confidential miRNA prediction, we identified miRNA based on formerly established criteria (Xia et al., 2015a; Axtell and Meyers, 2018; Chen et al., 2019). miRNAminerCLI from sRNAminer was used to annotate miRNAs based on sorted mapping files. The default parameters were used and listed below: the space size between miRNA and miRNA* was 5- to 300-nt, the length of mature miRNA was between 20- and 22-nt, sRNAs with more than 20 hits in genome which are supposed to be repeated sequences were filtered, the minimal abundance of

Table 1 The information of sRNA and degradome data

Reference	Scientific name	Line	Run number	Accession number	Library strategy	Specific stage
Xia et al., 2015	*Fragaria vesca*	Yellow Wonder 5AF7	SRR1586419	GSE61798	sRNA-Seq	4DPA ovary wall
			SRR1586420	GSE61798	sRNA-Seq	10DPA ovary wall
			SRR1586421	GSE61798	sRNA-Seq	4DPA seeds
			SRR1586422	GSE61798	sRNA-Seq	10DPA seeds
			SRR1586423	GSE61798	sRNA-Seq	10DPA receptacles
			SRR1586424	GSE61798	sRNA-Seq	Unopen flowers
			SRR1586425	GSE61798	sRNA-Seq	Unexpanded leaves
			SRR1586426	GSE61798	sRNA-Seq	4W seedling
			SRR1586427	GSE61798	PARE	Leaf and seedling-6MP
			SRR1586428	GSE61798	PARE	Open flower and flower bud-6MP
			SRR1586429	GSE61798	PARE	Achene and receptacle-6MP
Xia et al., 2013	*Fragaria vesca*		SRR771535	GSE44930	sRNA-Seq	Open flowers of 1D
			SRR771536	GSE44930	sRNA-Seq	Open flowers of 1D
			SRR771537	GSE44930	sRNA-Seq	Open flowers of 1D
Xia et al., 2019	*Fragaria vesca*	*Fragaria vesca*	SRR7250917	SRP149613	sRNA-Seq	Anthers of stage_6_S1
			SRR7250918	SRP149613	sRNA-Seq	Anthers of stage_7_S2
			SRR7250919	SRP149613	sRNA-Seq	Anthers of stage_8_S3
			SRR7250920	SRP149613	sRNA-Seq	Anthers of stage_9_S4
Šurbanovski et al., 2016	*Fragaria vesca* subsp. *vesca*	Hawaii-4	SRR2003391	PRJNA282518	sRNA-Seq	Stolons of 8WP
			SRR2003393	PRJNA282518	sRNA-Seq	Open flowers of 8WP
			SRR2003394	PRJNA282518	sRNA-Seq	Fruits of 8WP
			SRR2003395	PRJNA282518	PARE	mixed stages
	Fragaria vesca		SRR2003396	PRJNA282518	sRNA-Seq	Leaves of 8WP

Note: DPA. Days post anthesis; WP. Week-old plants; MP. Months plant; D. Day-opening; W. Week old plants. Shaded are PARE libraries.

miRNA was 10, cutoff of miRNA and miRNA* reads accounting for total reads was 0.75, the proportion of mapped reads located on the sense strand of the precursor was more than 90%. DetectKnownMiR was used to annotate known strawberry miRNAs (less than four mismatches), the rest potential miRNAs were annotated as novel miRNAs.

After that, we did manual check as described below. First, bam files (Li et al., 2009a) were loaded into IGV-sRNA (Chen et al., 2019) for viewing the sRNA mapping in each *MIR* loci (Robinson et al., 2011). Generally, *MIR* locus has only two read peaks, of which the higher one represents the miRNA while the other one denotes the miRNA*, and both of them are derived from the sense strand. Second, the Vienna RNA package was used for folding the precursor sequences of all potential miRNAs (Hofacker, 2003). Revised criteria of miRNA annotation were applied to screen miRNA secondary hairpin structure where five mismatches and three nucleotides in asymmetric bulges are maximum (Axtell and Meyers, 2018). For certain *MIR* locus, the miRNA* whose abundance is more than 30% of the sum of miRNA and miRNA* abundance was retained for subsequent analysis. Known miRNAs were named based on homology (Kozomara et al., 2018) and "miRN" was used as a prefix for denoting novel miRNAs.

2.4. *PHAS loci identificaion*

Identification of *PHAS* loci is based on *P*-value calculation, which was developed and modified in previous researches (de Paoli et al., 2009; Xia et al., 2013). PHASMinerCLI was used to predict *PHAS* loci. The parameters were as below, the length of siRNA with most abundance was either 21 or 24, the maximum *P*-value was 0.001, the abundance ratio of in-phase siRNAs was more than 0.3 and the minimum length of *PHAS* locus was 100 bp. The *PHAS* loci with max phasing score higher than 15 were characterized as confident *PHAS* loci. *PHAS* loci along with 200 bp flanking sequences (100 bp for each stream) were used to seek the target sites of potential triggering miRNAs. TargetSoPipe from sRNAminer was used to identify the trigger miRNA of *PHAS* loci with a maximum penalty score of five and a maximum mismatch of six. IGV-sRNA was used to distinguish *PHAS* loci from *MIR* loci based on the fact that sRNAs generated from *PHAS* loci are mapped to both strands. SWISS-PROT protein sequence database was used to annotate filtered *PHAS* loci (Bairoch and Apweiler, 2000; Camacho et al., 2009).

2.5. *Identification of target genes for miRNAs and phasiRNAs*

Adaptor sequences were removed from degradome data the same way as sRNA data. Then clean data were analyzed via CleaveLand4.0 to identify target miRNA transcripts (Brousse et al., 2014). Target sites satisfied with the confident level of category 0 to 2 and with alignment penalty score less than or equal to 5 were selected as credible miRNA cleave sites. The rest target genes that belong to category 3 and 4 were neglected. The

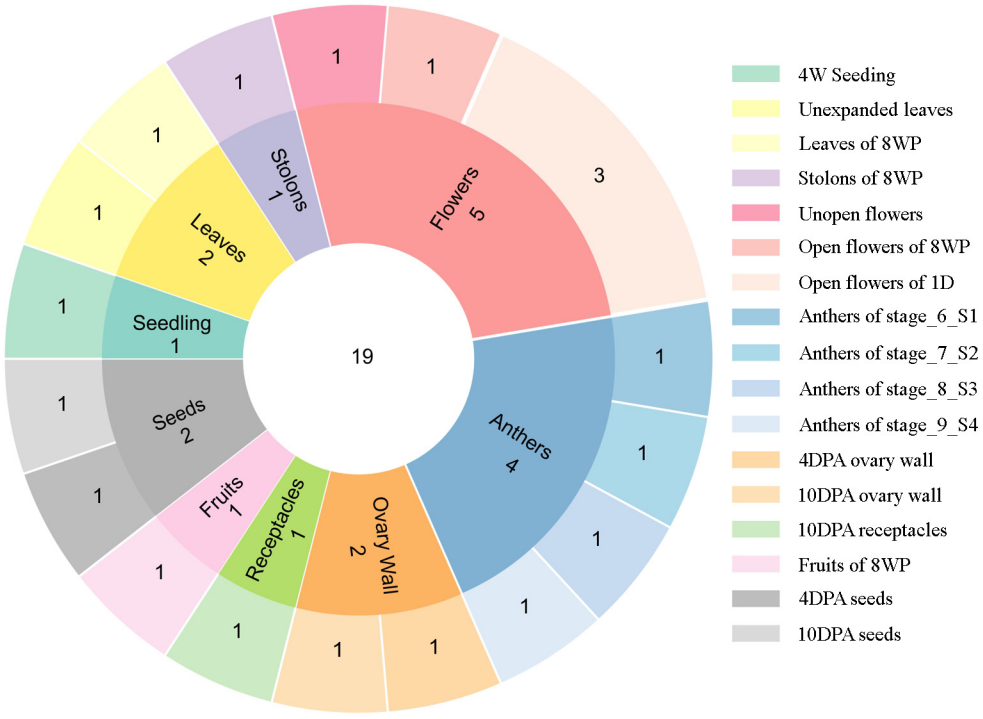

Fig. 1 The statistics of collected sRNA sequencing data

The inner circle denotes the tissue of each library while the outer circle indicates detailed information of each library. W: Week; WP: Week-old plant; D: Day-opening; DPA: Days post anthesis; S1–S4: Different developmental stage of anthers referred to Xia et al. (2019).

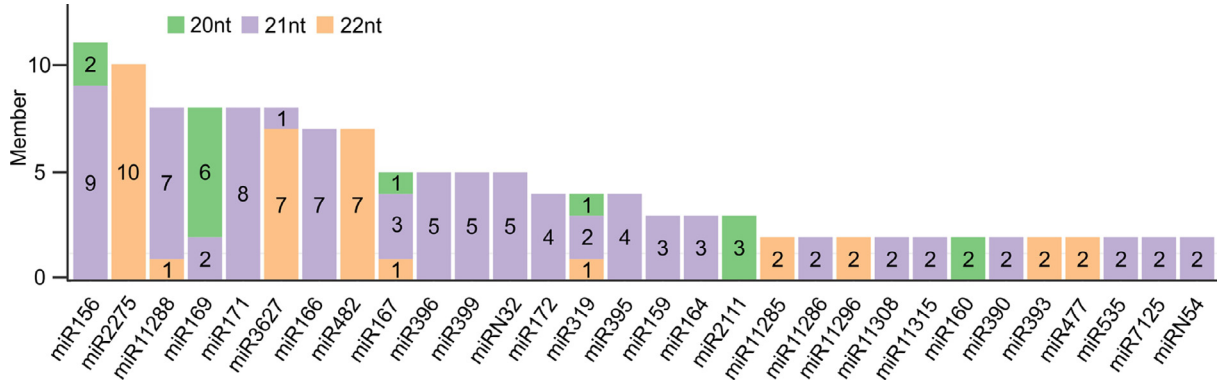

Fig. 2 The number of members in each miRNA family

The length of each miRNA family member is indicated in different colors. Green denotes 20-nt miRNA, purple 21-nt miRNA and orange 22-nt miRNA.

gene ontology category was performed using TBtools (Chen et al., 2018a).

3. Results

3.1. *Re-annotation of strawberry miRNAs*

To get a reliable annotation of strawberry miRNAs, we firstly collected sRNA sequencing data from 19 published libraries, which include five libraries from flowers, four from anthers, two from ovary walls, one from receptacles, one from fruits, two from seeds, one from seedlings, two from leaves and one from stolons (Fig. 1). After filtering low quality reads and trimming adaptor sequences, all sRNAs sequences were mapped to the latest *F. vesca* genome (V4.0) via bowtie while the digital expression of each sRNA was calculated by reads per 10 million (RP10M). To annotate miRNAs, we referred to the latest criteria revised by Axtell et al. (2018), followed by manual check.

As a result, 167 known miRNAs belonging to 70 families were identified, 37 out of 70 were conserved or less-conserved miRNA families and the rest 33 known miRNA families were identified recently and seemed to be specific in strawberry (with annotation accession from miR11283 to miR11315). Among known miRNAs, 30 of them were generated from at least two loci (Fig. 2). miR156 family is the biggest family in strawberry, which owns

11 family members derived from 11 different loci in strawberry genome (Fig. 2, Table S1). Besides, miR166, miR169, miR171, miR482, miR2275, miR3627 and miR11288 also have more than six family members. In addition, we annotated 27 known miRNA stars that haven't been degraded in strawberry. Their mature sequences were retained in strawberry with significant abundance and might be functional as miRNA. For novel miRNAs annotation, the detection of miRNA* expression is required. If novel miRNAs in both strands of duplexes confer notable abundance (30% of total reads of miRNA and miRNA*), we will name them with suffix −3p and −5p, such as miRN40-3p and miRN40-5p. Consequently, 54 novel *MIR* genes were identified. Interestingly, miRN32 has five loci in the strawberry genome (Fig. 2). While manual check, we found two known strawberry miRNAs were mis-annotated. The first is fve-miR477b, whose sequence is totally different from the other miR477, such as fve-miR477a/c, vvi-miR477b, mdm-miR477a, etc., meanwhile fve-miR477a/c and fve-miR477b target different transcripts in strawberry (Fig. 3, a). The second case is fve-miR5225, who presents the consensus sequence with fve-miR3627 family members, and targets the same transcripts as fve-miR3627a/b (Fig. 3, b). Thus, we renamed fve-miR477a and fve-miR5225 as fve-miRN47 and fve-miR3627h respectively. In addition, the features (including position information of precursor, mature miRNA and miRNA*) of all *MIR* genes were described in a GFF file (Supplemental File 1).

3.2. *The regulatory roles of strawberry miRNA*

After identification of miRNAs from 19 strawberry sRNA libraries, we get the expression matrix (calculated as reads per 10 million, RP10M) of all miRNAs from different strawberry tissues (Table S1). To get a clear expression pattern of all miRNAs in different tissues (17 different tissues from 19 libraries), we drew heat maps for known and novel miRNAs respectively by hierarchical clustering and Z-score normalization (Figs. 4, 5). As a result, we found that a bunch of miRNAs showed tissue-specific or tissue-preferential expression. For example, miR2275 family and miR393a are specifically expressed in anthers (Fig. 6, a). miR3627 family are highly expressed in unexpanded leaves (Fig. 6, b). miR164c is accumulated mainly in the ovary wall (Fig. 6, c). miR11289, miR11292, miR11303, and miR167e reveal high accumulation in seeds (Fig. 6, d). The top three abundant novel miRNAs are miRN04, miRN09, miRN40 (Table S1). Interestingly, we found miRN04 and miRN09 showed specific accumulation in anthers (Table S1). The expression of miRN04 is continuously accumulating while miRN09 is decreasing during the development of anthers. Besides, miRN08, miRN13, miRN14, miRN16, miRN18, miRN28, and miRN33 also showed preferential expression in anthers (Fig. 6, e, Table S1). miRN39 and miRN44-3p preferentially expressed in the ovary wall (Fig. 6, f). In most libraries, the expression level of miRN40-5p was higher than miRN40-3p. But in ovary wall,receptacle and 10 DPA seeds, miRN40-3p showed higher expression level than miRN40-5p, indicating that miRNAs from different arms of certain precursor might accumulate preferentially in different tissues (Table S1).

To investigate the biological functions of strawberry miRNAs, we identified target genes for all miRNAs using four degradome sequencing data (detailed information Table 1). 1 530 target genes were identified and classified into five categories (category 0 to 4, category 0 possesses the highest confidence level) according to CleaveLand 4.0 pipeline. Out of them, 634 target genes from category 0, 1 and 2 were used for further analysis. Functional annotations were further performed to investigate which processes of strawberry miRNAs are predomi-

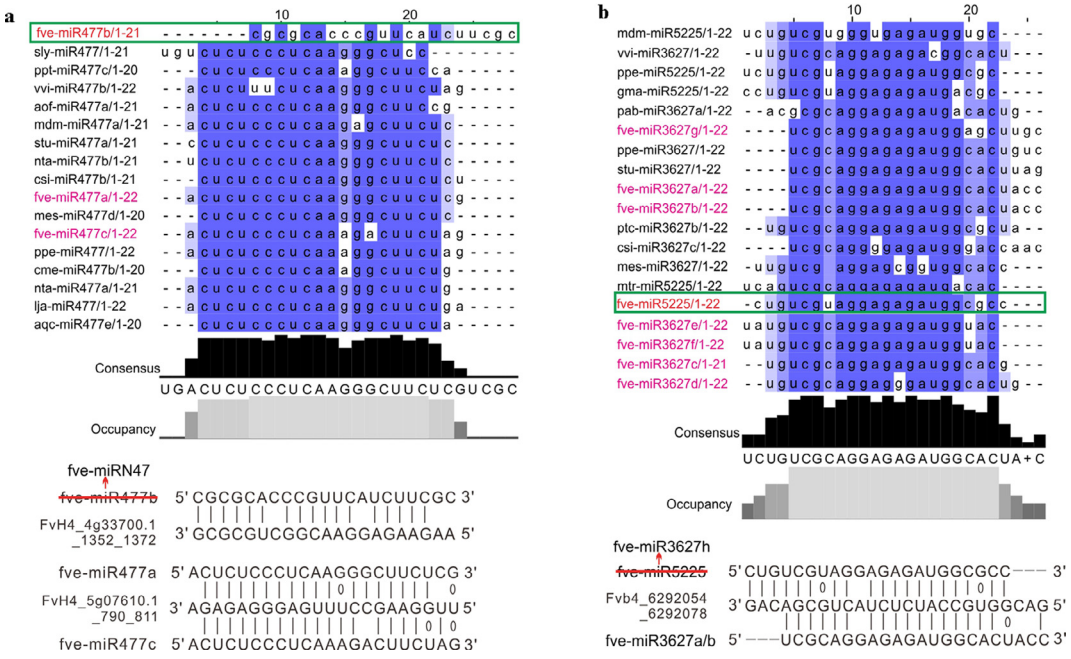

Fig. 3 Correction of two mis-annotated miRNAs

Multiple sequence alignment was applied by Clustal Omega and viewed in Jalview. The mis-annotated miRNAs are highlighted in red. Other family members of miR477 and miR3627 are highlighted in magenta. a. Rename of miRN47, b. Rename of miR3627h.

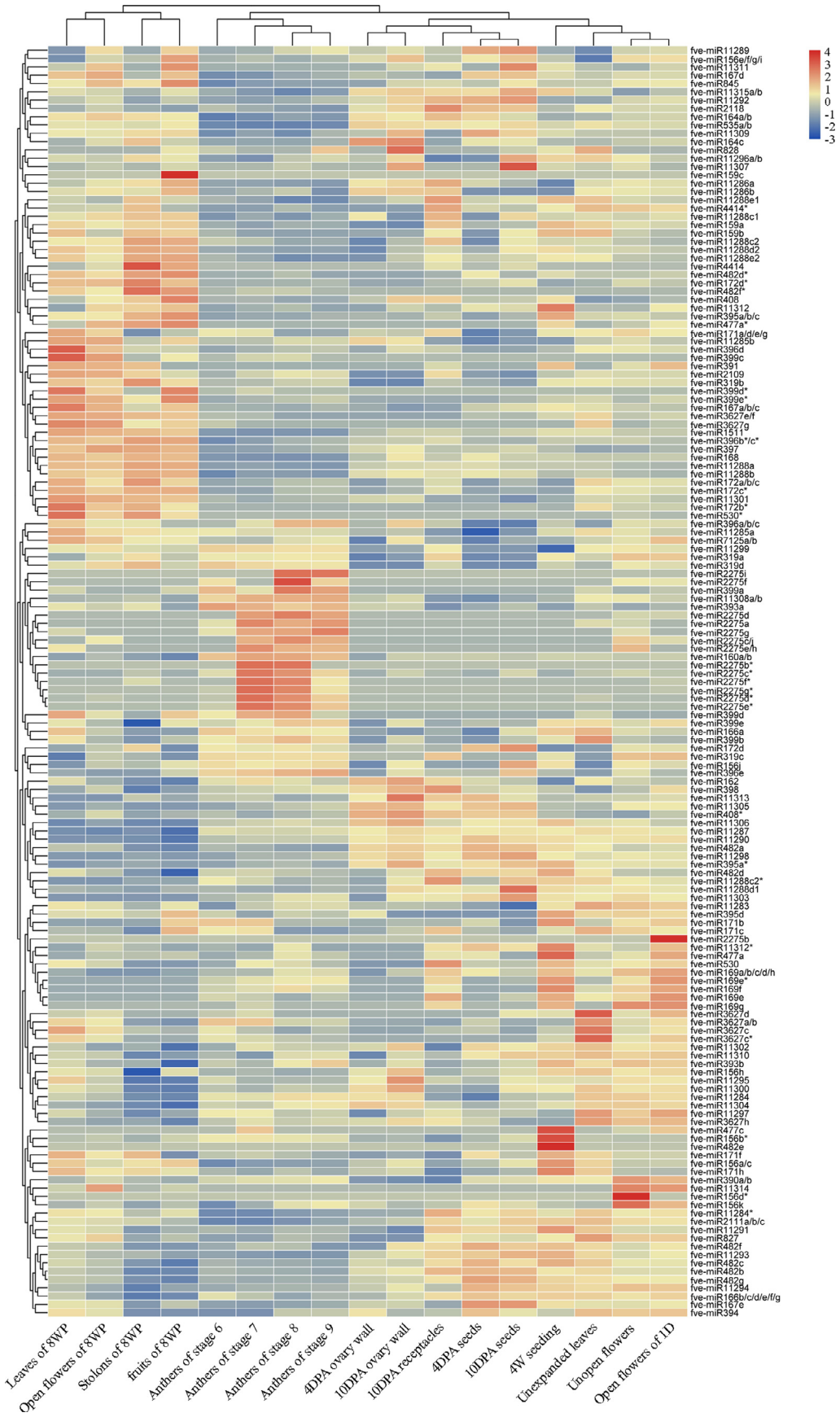

Fig. 4 Heatmap of known miRNAs in 17 libraries

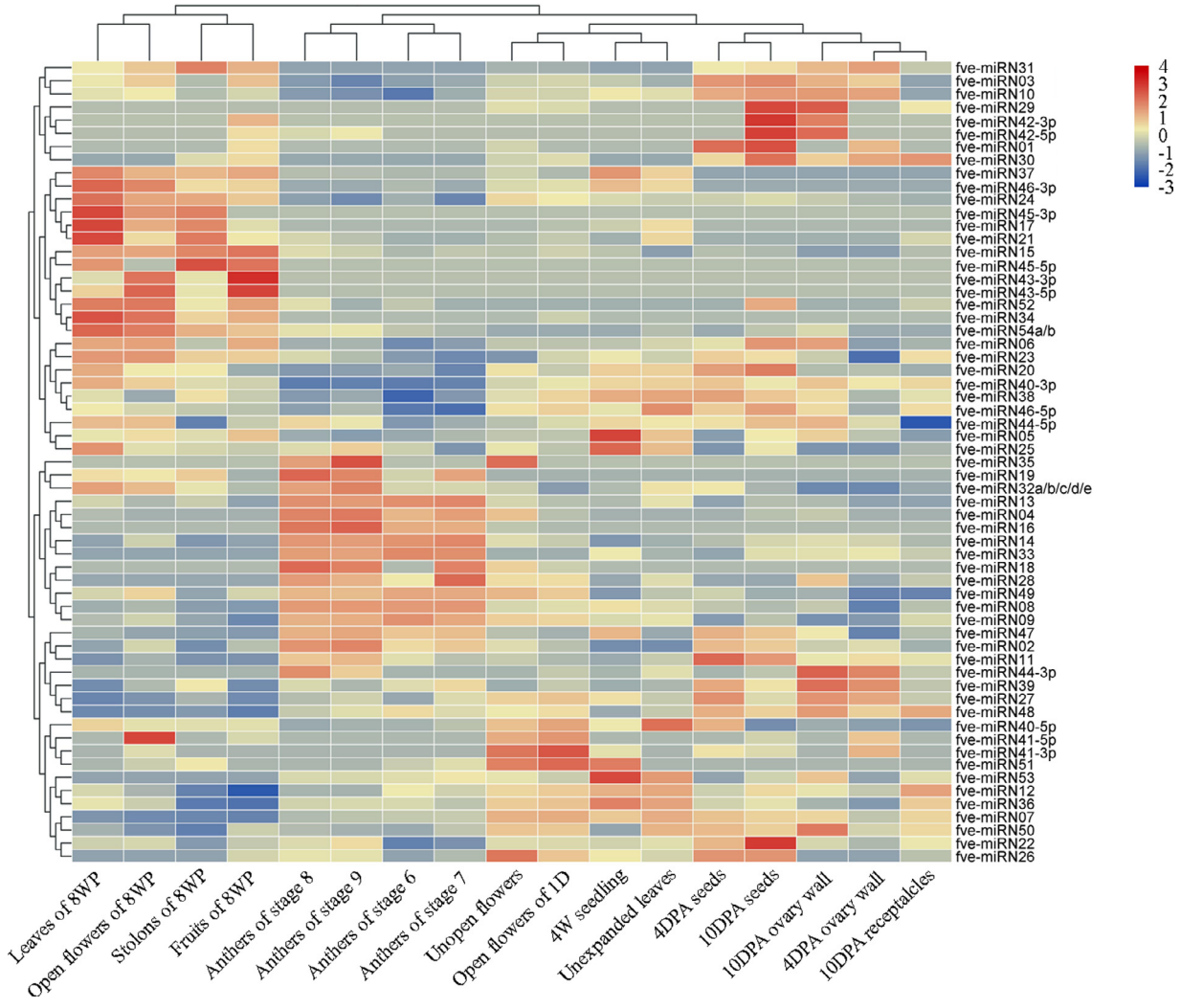

Fig. 5 Heatmap of novel miRNAs in 17 libraries

nantly involved in Table S2. Accordingly, most conserved miRNA-directed regulatory pathways were identified via our analysis, such as miR156-*SQUAMOSA PROMOTER BINDING PROTEIN-LIKE* (*SPL*) genes, miR159-*MYB*s, miR164-*NAC*s, miR167- auxin response factor (*ARF*) genes, miR168-*AGO* gene and miR482-disease resistance genes (Table S2). Interestingly, miR164a/b and miR164c, between whom there were only two different nucleotides (Table S1), were found to regulate different *NAC* genes (Table S2). Moreover, miR164a/b and miR164c showed different expression pattern around different tissues (Fig. 6, c). All these observations indicated that miR164a/b and miR164c might be differentiated functional. Strawberry novel miRNAs might be recently evolved and presented novel target genes. For example, miRN09 regulates the expression of cytokinin dehydrogenase coding genes, miRN26 targets F-box protein coding genes (Table S2). To evaluate the potential roles of all miRNAs targeted genes in strawberry, gene ontology (GO) was assigned to categorize target genes according to the cellular component, molecular function, and biological process. Based on biological process, all target genes were grouped into 14 categories, the top three over-represented GO terms are response to stress, anatomical structure development and response to chemical. The most three frequent terms based on molecular function are protein binding, transferase activity and DNA-binding transcription factor activity (Fig. 7). Besides targeting coding genes, 32 strawberry miRNAs are capable of regulating 42 non-coding transcripts simultaneously. Unexpectedly, two miRNAs (miR2275c* and miRN36) seem to target two non-coding RNAs (category 2 targets) exclusively. Only 5 of 44 ncRNA targets belong to category 0 targets, suggesting most of these target genes need further validation. Several ncRNA targets function as substrates of phasiRNA biogenesis, such as *TAS3* targeted by miR390, the five ncRNAs targeted by miR482 (Table S2).

3.3. *Annotation of strawberry* PHAS *loci*

Some strawberry miRNAs are 22-nt, such as miR2275, miR482, miR393, miR3627 and miR11288 (Fig. 2), which might be capable of triggering phasiRNA biogenesis. After manual check, 192 *PHAS* loci producing 21-nt phasiRNAs with maximum phasing score larger than 15 were selected for further study (Supplemental File 2). Among them, 110 *PHAS* loci were triggered by miRNAs (Table S3). The rest *PHAS* loci lacking consistent miRNA triggers might be processed by unknown mechanisms. In total,

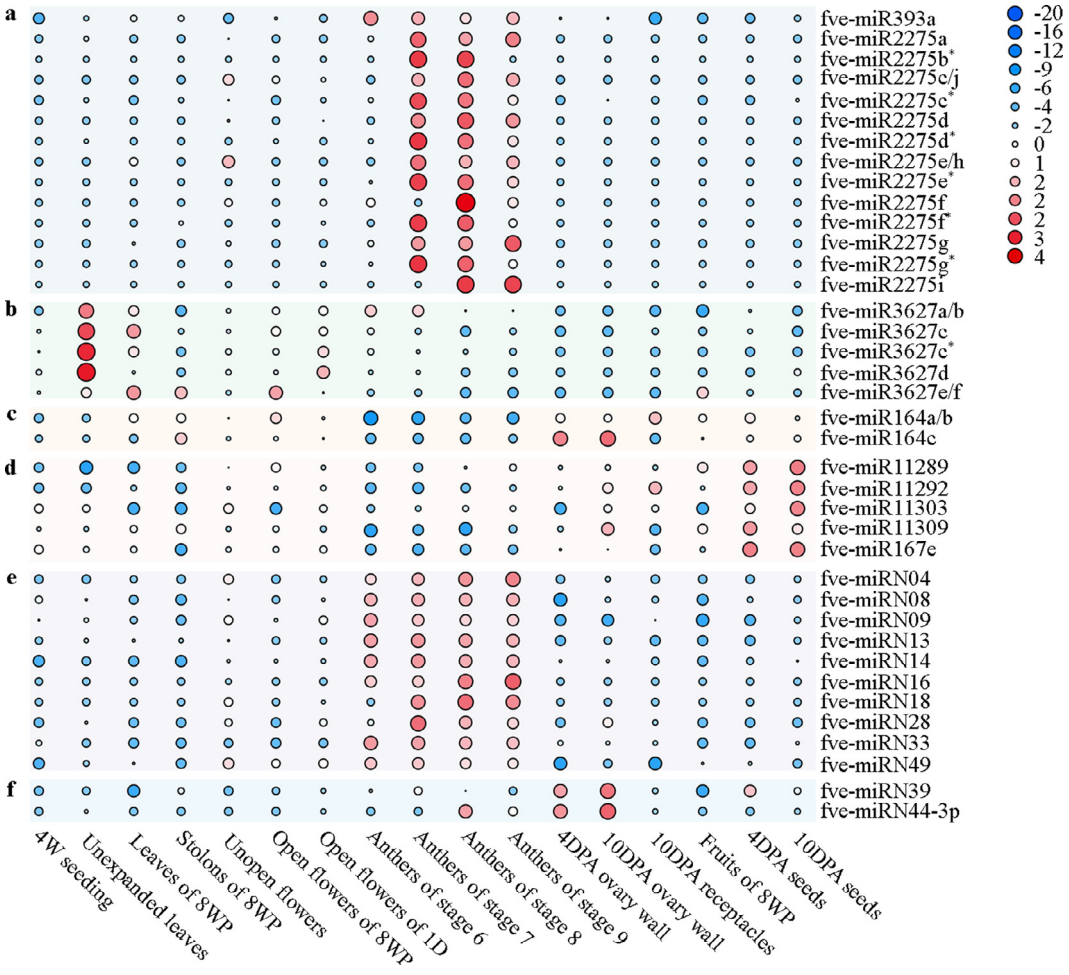

Fig. 6 Heatmap of tissues preferentially expressed miRNAs

The heatmap was drawn based on the digital expression data. The color bar is shown at the right side of the panel. Known miRNAs preferentially expressed in anthers(a), leaves (b), ovary wall (c) and seeds (d). Novel miRNAs preferentially expressed in anthers (e) and ovary wall (f).

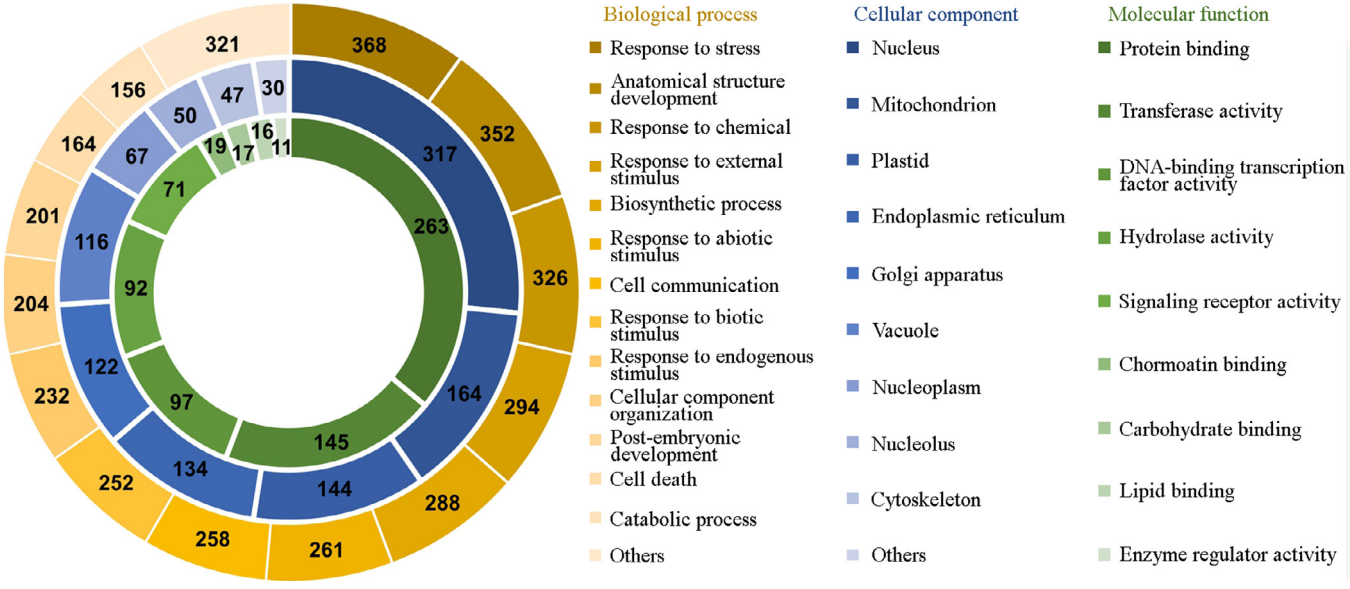

Fig. 7 Gene ontology categories of all strawberry miRNAs target genes

Categorization of miRNA target genes was applied according to biological process, cellular component, and molecular function.

12 miRNAs (miR11285, miR11288, miR11293, miR2109, miR2118, miR3627, miR390, miR393, miR482, miR828, miRN09, and miRN33) were identified as triggers. Among these 110 *PHAS* loci, 83 *PHAS* are protein coding genes, including disease resistance genes targeted by miR482/miR2109, F-box protein coding genes targeted by miR11288, pentatricopeptide repeat-containing protein (*PPR*) coding genes targeted by miR11285, calcium-transporting ATPase coding genes targeted by miR3627, bHLH coding genes/auxin signaling F-box genes targeted by miR393, *MYB* targeted by miRN33, cytokinin dehydrogenase coding genes targeted by miRN09 (Table S3). 27 *PHAS* loci were annotated as noncoding transcripts, which might act as substrates producing phasiRNAs regulating downstream genes *in trans*. Additionally, 323 *PHAS* producing 24-nt phasiRNAs were annotated in GFF file based on genome position (Supplemental File 3). Among them, 225 *PHAS* loci generating 24-nt phaisRNAs were triggered by miR2275 in strawberry (Table S5).

Later on, we also checked the expression of all small RNAs from each *PHAS* loci (Fig. 8). Notably, small RNAs from *PHAS* loci (*Fvb6_2720273_2721068*, *Fvb6_2716681_2717725* and *Fvb6_3417771_3418603*) targeted by miRN09 were accumulated at a higher level at anthers, which is consistent with the expression pattern of miRN09. Small RNAs from *PHAS* locus (*Fvb3_12138147_12138591*) targeted by miR11288e1 specifically expressed in seeds, however, the trigger miR11288e1 was present in almost all tissues and showed no tissue preference. A reasonable explanation is that the *PHAS* locus (*Fvb3_12138147_12138591*) specifically expressed in seeds. These findings indicated that the expression pattern of phasiRNAs depends on the expression of both the miRNA trigger and *PHAS* locus. Subsequently, we obtained top 10 abundant sRNA derived from each *PHAS* loci from different tissues and used degradome data to identify the downstream regulated genes. Hence, 2446 transcripts that were involved in many aspects of biological processes were regulated by phasiRNAs *in cis* or *in trans* (Table S4), indicating that miRNA trigger and their *PHAS* loci work together and amplify silencing effect of miRNAs.

3.4. *"Two-hit" phasiRNA biogenesis model in strawberry*

As mentioned above, there are two models of phasiRNA biogenesis, "one-hit" model for almost all 22-nt miRNA trigger and "two-hit" model for the miR390-*TAS3* pathway. In most vascular plants, 5′ proximal miR390 target site on *TAS3* is non-cleavable while 3′ proximal target site is sufficient for miR390-directed slicing, leading to a "two-hit, one-cleavage" model (Xia et al., 2017). The cleavable site provides the initial position for phasiRNA biogenesis while the non-cleavable site acts as a "definer" to determine the region for phasiRNA biogenesis, providing a much more accurate way to generate phasiRNAs (Felippes et al., 2017). In the strawberry genome, besides miR390-directed "two-hit" model, we found that miR11285a and miRN40-3p co-targeted *PHAS* locus *Fvb3_30369442_30370735*, miR397 and miR482a co-targeted *PHAS* locus *Fvb3_37130354_37131719* (Fig. 9). Both miR11285a and miRN40-3p target site in *Fvb3_30369442_30370735* are cleavable with 3.5 and 2.5 penalty score respectively. miR11285a is 22-nt in length while miRN40-3p is 21-nt in length. In this case, 22-nt miR11285a may work as the phasiRNA trigger and 21-nt miRN40-3p-directed slicing defines the end of the phasiRNA generating region. Within the defined region between two target sites, sRNAs were generated in phase initiating from the miR11285a cleavage site towards miRN40-3p cleavage site (Fig. 9, a). Almost no sRNA were mapping out of the defined region. It is reasonable to speculate that miR11285a and miRN40-3p collaborate together to form a "two-hit" like model as miR390 does. Similarly, 22-nt miR482a and 21-nt miR397 act as phasiRNA trigger and "definer" respectively in *Fvb3_37130354_37131719* and trigger the phasiRNA biogenesis within the defined region (Fig. 9, b).

4. Discussion

4.1. *miRNA* might be functional*

miRNA* was supposed to act as miRNA carrier and be degraded after unwinding from miRNA/miRNA* duplex. However, there are a few studies demonstrating that miRNA* associated with AGO guided the silencing of downstream genes, indicating that miRNA* may function as miRNA does (Zhang et al., 2011). In our study, besides known miRNA and novel miRNA, we annotated 27 miRNA*s that have significant abundance. The rest 140 miRNA*s are absent or express at an extremely low level in most libraries. These findings indicate that these 27 miRNA*s might be selected and kept to participate in certain biological process, instead, guide miRNAs might be degraded (Kobayashi and Tomari, 2016). Even miRNA* has high abundance, it doesn't mean that it could function as mature miRNAs. Most functional plant miRNAs have a 5′ terminal nucleotide "U" as their partner AGO1 prefers to bind small RNAs with a 5′ "U" to form a slicing complex (Kim, 2008). Out of 27 miRNA*, only 5 miRNA*s start with 5′ U. A reasonable speculation is that these miRNA*s may bind other AGOs to form a RISC. We also used degradome data to identify target genes for these miRNA*. Fifty-nine target genes (belong to category 0, 1 and 2) were predicted. Only 4 of them belong to category 0 and 1, indicating the function of these high abundant miRNA stars remain largely unclear.

4.2. *Manual check is essential for sRNA annotation*

With the development of sequencing technology, the cost of high-throughput sequencing is drastically reduced, leading to an outbreak of sRNA sequencing data. A bunch of scripts or pipelines were developed for miRNA annotation. Most data were processed by these pipelines and published directly without manual check, leading to poor annotation. More and more poor annotation may compromise the confidence of miRNA deposited in miRbase. As we know, conserved miRNA annotation is based on blasting against miRbase dataset, leading to vicious circle in miRNA annotation. Taking fve-miR477b in miRbase as an example, the sequence of fve-miR477b is totally different from the other miR477 registered in miRbase. It should be a new accession in miRbase. If it hasn't been corrected, its homologs from other species may be also annotated as miR477. Thus, manual checking each *MIR* gene one by one is highly recommended.

4.3. *Novel "two-hit" PHAS loci in strawberry*

The biogenesis of phasiRNA has been well studied in the past decade. 22-nt miRNA-directed "one-hit" model is prevalent

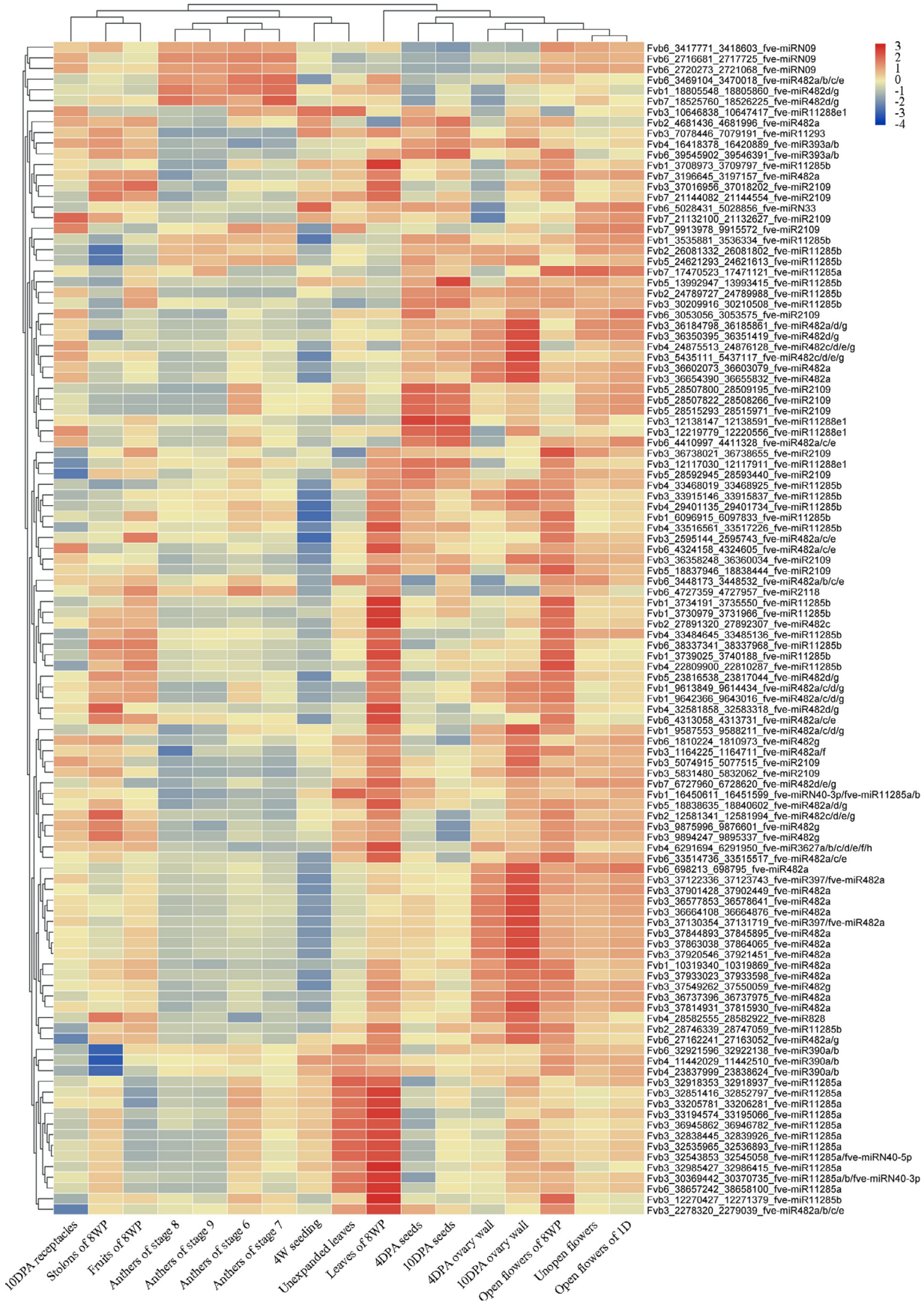

Fig. 8 Heatmap of phasiRNA from 110 *PHAS* loci in 17 libraries

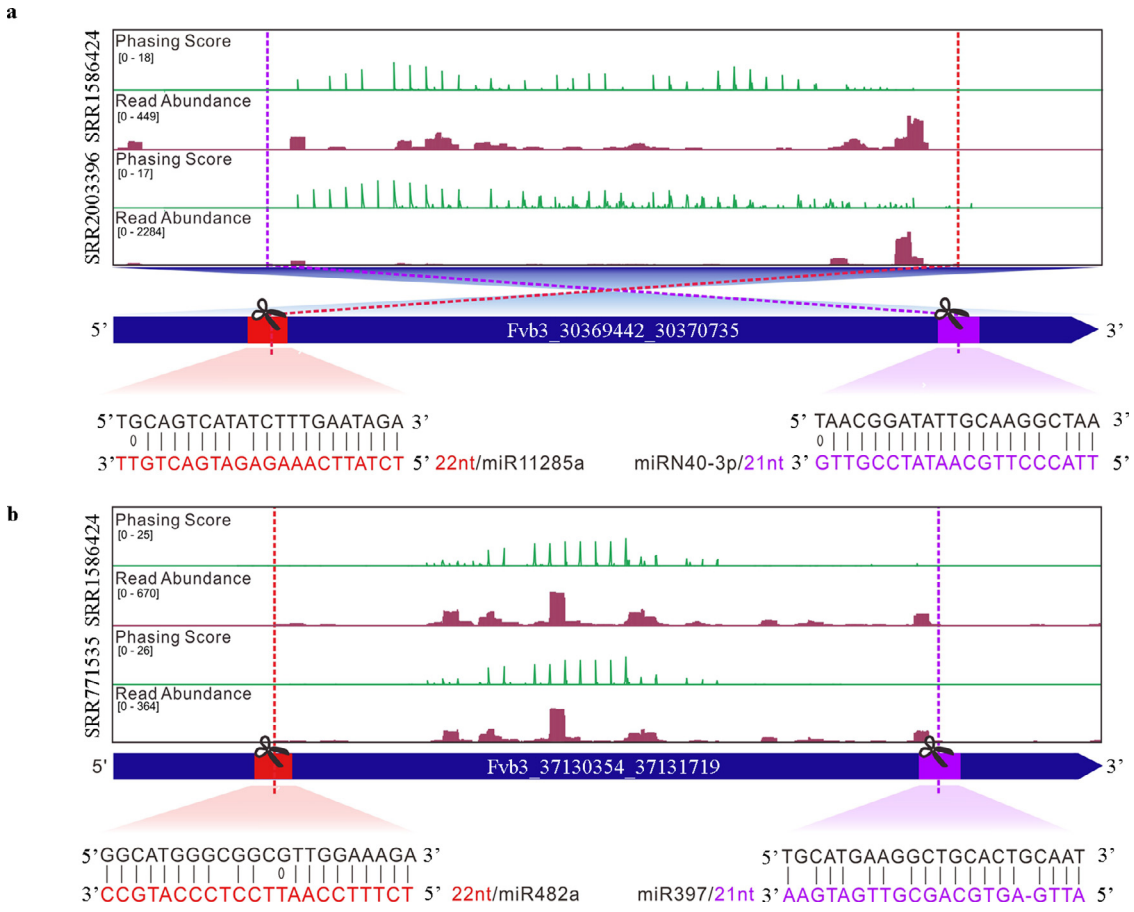

Fig. 9 *PHAS* loci generate phasiRNAs via "two-hit" like model in strawberry

Phasing score and sRNA abundance are viewed in IGV-sRNA at the *PHAS* loci that is co-targeted by two miRNAs. The red dashed lines and rectangle indicate the slicing site and target sites of 22-nt miRNAs respectively while the purple dashed lines and rectangle indicate the slicing site and target sites of 21-nt miRNAs. a. IGV-sRNA view of the *PHAS* locus *Fvb3_30369442_30370735*. b. IGV-sRNA view of the *PHAS* locus *Fvb3_37130354_37131719*.

for producing phasiRNA across plant kingdom. In contrast, 21-nt miR390 along with its specialized partner AGO7 seem to be the only trigger of phasiRNA biogenesis via "two-hit" model (Fei et al., 2013). Actually, a previous study demonstrated that "one-hit" was sufficient for miR390 triggering the phasiRNA biogenesis (Felippes et al., 2017). However, the configuration of "two-hit, one-cleavage" may provide a better-defined region to generate phasiRNAs. Moreover, in "two-hit" model, 3′ proximal target site is cleavable and upstream sequence of degraded fragment was retained, leading to trimming off the poly(A) tail of *TAS3*, which may facilitate the recruitment of RDR6 for dsRNA conversion (Baeg et al., 2017). These findings suggest that "one-hit" model may be a fundamental model for phasiRNA biogenesis while "two-hit" model is adapted to generate accurate phasiRNAs to specifically regulate downstream genes (Felippes et al., 2017). In our study, we found two cases that two miRNAs (one is 22-nt, the other is 21-nt) target a common transcript and trigger the phasiRNA biogenesis between two target sites. In both cases, 22-nt miRNA-mediated slicing happens on the 5′ end, playing a role as phasiRNA trigger like regular 22-nt miRNA does in "one-hit" model. 21-nt miRNA-mediated cleavage locates on the 3′ end, acting as a "definer" providing the terminus of phasiRNA biogenesis region. Meanwhile, 3′ end cleavage trims poly(A) tail which may be helpful for RDR6 recruitment. These observations provide insight that "two-hit" model may be adopted by other miRNAs rather than miR390.

Acknowledgments

This work was supported by the National Natural Science Foundation of China (Grant No. 31872063).

Supplementary materials

Supplementary material associated with this article can be found, in the online version, at doi:10.1016/j.hpj.2019.11.004.

REFERENCES

Achkar, N.P., Cambiagno, D.A., Manavella, P.A., 2016. miRNA biogenesis: a dynamic pathway. Trends Plant Sci, 21: 1034–1044.

Axtell, M.J., 2013. Classification and comparison of small RNAs from plants. Annu Rev Plant Biol, 64: 137–159.

Axtell, M.J., Jan, C., Rajagopalan, R., Bartel, D.P., 2006. A two-hit trigger for siRNA biogenesis in plants. Cell, 127: 565–577.

Axtell, M.J., Meyers, B.C., 2018. Revisiting criteria for plant miRNA annotation in the era of big data. Plant Cell, 30: 272–284.

Baeg, K., Iwakawa, H., Tomari, Y., 2017. The poly(A) tail blocks RDR6 from converting self mRNAs into substrates for gene silencing. Nat Plants, 3: 17036.

Bairoch, A., Apweiler, R., 2000. The Swiss-port protein sequence database and its supplement Trembl in 2000. Nucleic Acids Res, 28: 45–48.

Bartel, D.P., 2004. MicroRNAs: genomics, biogenesis, mechanism, and function. Cell, 116: 281–297.

Brousse, C., Liu, Q., Beauclair, L., Deremetz, A., Axtell, M.J., Bouché, N., 2014. A non-canonical plant microRNA target site. Nucleic Acids Res, 42: 5270–5279.

Cai, Q., Qiao, L., Wang, M., He, B., Lin, F., Palmquist, J., Jin, H., 2018. Plants send small RNAs in extracellular vesicles to fungal pathogen to silence virulence genes. Science, 360: 1126–1129.

Camacho, C., Coulouris, G., Avagyan, V., Ma, N., Papadopoulos, J., Bealer, K., Madden, T.L., 2009. BLAST^{+}: architecture and applications. BMC Bioinform, 10: 421.

Chen, C., Feng, J., Liu, B., Li, J., Feng, L., Yu, X., Zhai, J., 2019. sRNAanno–a database repository of uniformly-annotated small RNAs in plants. bioRxiv, doi:10.1101/771121.

Chen, C., Xia, R., Chen, H., He, Y., 2018a. TBtools, a toolkit for biologists integrating various HTS-data handling tools with a user-friendly interface. bioRxiv, doi:10.1101/289660.

Chen, C., Zeng, Z., Liu, Z., Xia, R., 2018b. Small RNAs, emerging regulators critical for the development of horticultural traits. Hortic Res, 5: 63.

Chen, H., Chen, L., Patel, K., Li, Y., Baulcombe, D.C., Wu, S., 2010. 22-Nucleotide RNAs trigger secondary siRNA biogenesis in plants. Proc Natl Acad Sci, 107: 15269–15274.

Cho, S.H., Coruh, C., Axtell, M.J., 2012. miR156 and miR390 regulate tasiRNA accumulation and developmental timing in *Physcomitrella patens*. Plant Cell, 24: 4837–4849.

Cui, H., Tsuda, K., Parker, J.E., 2015. Effector-triggered immunity: from pathogen perception to robust defense. Annu Rev Plant Biol, 66: 487–511.

Cuperus, J.T., Carbonell, A., Fahlgren, N., Garcia-Ruiz, H., Burke, R.T., Takeda, A., Sullivan, C.M., Gilbert, S.D., Montgomery, T.A., Carrington, J.C., 2010. Unique functionality of 22-nt miRNAs in triggering RDR6-dependent siRNA biogenesis from target transcripts in *Arabidopsis*. Nat Struct Mol Biol, 17: 997–1003.

D'Ario, M., Griffiths-Jones, S., Kim, M., 2017. Small RNAs: big impact on plant development. Trends Plant Sci, 22: 1056–1068.

De Paoli, E., Dorantes-Acosta, A., Jixian, Z., Accerbi, M., Jeong, D.H., Sunhee, P., Meyers, B.C., Jorgensen, R.A., Green, P.J., 2009. Distinct extremely abundant siRNAs associated with cosuppression in *Petunia*. RNA, 15: 1965–1970.

Dong, Q.H., Han, J., Yu, H.P., Wang, C., Zhao, M.Z., Liu, H., Ge, A.J., Fang, J.G., 2012. Computational identification of microRNAs in strawberry expressed sequence tags and validation of their precise sequences by miR-RACE. J Hered, 103: 268–277.

Fei, Q., Xia, R., Meyers, B.C., 2013. Phased, secondary, small interfering RNAs in posttranscriptional regulatory networks. Plant Cell, 25: 2400–2415.

Fei, Q., Zhang, Y., Xia, R., Meyers, B.C., 2016. Small RNAs add zing to the Zig-Zag-Zig model of plant defenses. Mol Plant Microbe Interact, 29: 165–169.

Felippes, F.F., Marchais, A., Sarazin, A., Oberlin, S., Voinnet, O., 2017. A single miR390 targeting event is sufficient for triggering *TAS3*-tasiRNA biogenesis in *Arabidopsis*. Nucleic Acids Res, 45: 5539–5554.

Ge, A., Shangguan, L., Zhang, X., Dong, Q., Han, J., Liu, H., Wang, X., Fang, J., 2013. Deep sequencing discovery of novel and conserved microRNAs in strawberry (*Fragaria* × *ananassa*). Physiol Plant, 148: 387–396.

Guan, X., Pang, M., Nah, G., Shi, X., Ye, W., Stelly, D.M., Chen, Z.J., 2014. miR828 and miR858 regulate homoeologous *MYB2* gene functions in *Arabidopsis* trichome and cotton fibre development. Nat Commun, 5: 3050.

Guo, G., Liu, X., Sun, F., Cao, J., Huo, N., Wuda, B., Xin, M., Hu, Z., Du, J., Xia, R., Rossi, V., Peng, H., Ni, Z., Sun, Q., Yao, Y., 2018. Wheat miR9678 affects seed germination by generating phased siRNAs and modulating abscisic acid/gibberellin signaling. Plant Cell, 30: 796–814.

Han, J., Li, A., Liu, H., Wen, X., Zhao, M., Korir, N.B., Korir, N.K., Wang, C., Fang, J., 2014. Computational identification of microRNAs in the strawberry (*Fragaria* × *ananassa*) genome sequence and validation of their precise sequences by miR-RACE. Gene, 536: 151–162.

Hobecker, K.V., Reynoso, M.A., Bustos-Sanmamed, P., Wen, J., Mysore, K.S., Crespi, M., Blanco, F.A., Zanetti, M.E., 2017. The microRNA390/*TAS3* pathway mediates symbiotic nodulation and lateral root growth. Plant Physiol, 174: 2469–2486.

Hofacker, I.L., 2003. Vienna RNA secondary structure server. Nucleic Acids Res, 31: 3429–3431.

Hou, Y., Zhai, Y., Feng, L., Karimi, H.Z., Rutter, B.D., Zeng, L., Choi, D.S., Zhang, B., Gu, W., Chen, X., Ye, W., Innes, R.W., Zhai, J., Ma, W., 2019. A phytophthora effector suppresses trans-kingdom RNAi to promote disease susceptibility. Cell Host Microbe, 25: 153–165.

Kalvari, I., Nawrocki, E.P., Argasinska, J., Quinones-Olvera, N., Finn, R.D., Bateman, A., Petrov, A.I., 2018. Non-coding RNA analysis using the RFAM database. Curr Protoc Bioinform, 62: e51.

Kim, V.N., 2008. Sorting out small RNAs. Cell, 133: 25–26.

Kobayashi, H., Tomari, Y., 2016. RISC assembly: coordination between small RNAs and Argonaute proteins. Biochim et Biophys Acta (BBA)-Gen Regul Mech, 1859: 71–81.

Kozomara, A., Birgaoanu, M., Griffiths-Jones, S., 2018. miRBase: from microRNA sequences to function. Nucleic Acids Res, 47: D155–D162.

Langmead, B., 2010. Aligning short sequencing reads with Bowtie. Curr Protoc Bioinform, 32: 11.7.1–11.7.14.

Li, C., Li, Y., Bai, L., He, C., Yu, X., 2016. Dynamic expression of miRNAs and their targets in the response to drought stress of grafted cucumber seedlings. Hortic Plant J, 2: 41–49.

Li, D., Mou, W., Xia, R., Li, L., Zawora, C., Ying, T., Mao, L., Liu, Z., Luo, Z., 2019. Integrated analysis of high-throughput sequencing data shows abscisic acid-responsive genes and miRNAs in strawberry receptacle fruit ripening. Hortic Res, 6: 1–13.

Li, H., Handsaker, B., Wysoker, A., Fennell, T., Ruan, J., Homer, N., Marth, G., Abecasis, G., Durbin, R., 2009a. The sequence alignment/map format and SAMtools. Bioinformatics, 25: 2078–2079.

Li, H., Mao, W., Liu, W., Dai, H., Liu, Y., Ma, Y., Zhang, Z., 2013. Deep sequencing discovery of novel and conserved microRNAs in wild type and a white-flesh mutant strawberry. Planta, 238: 695–713.

Li, H., Zhang, Z., Huang, F., Chang, L., Ma, Y., 2009b. MicroRNA expression profiles in conventional and micropropagated strawberry (*Fragaria* × *ananassa* Duch.) plants. Plant Cell Rep, 28: 891–902.

Li, J., Yang, Z., Yu, B., Liu, J., Chen, X., 2005. Methylation protects miRNAs and siRNAs from a 3′-end uridylation activity in *Arabidopsis*. Curr Biol, 15: 1501–1507.

Li, S., Liu, J., Liu, Z., Li, X., Wu, F., He, Y., 2014. *HEAT-INDUCED TAS1 TARGET1* mediates thermotolerance via heat stress transcription factor A1a-directed pathways in *Arabidopsis*. Plant Cell, 26: 1764–1780.

Liang, Y., Guan, Y., Wang, S., Li, Y., Zhang, Z., Li, H., 2018. Identification and characterization of known and novel microRNAs in strawberry fruits induced by *Botrytis cinerea*. Sci Rep, 8: 10921.

Lin, Y., Lin, L., Lai, R., Liu, W., Chen, Y., Zhang, Z., Xu, H.X., Lai, Z., 2015. MicroRNA390-directed *TAS3* cleavage leads to the production of tasiRNA-*ARF3/4* during somatic embryogenesis in *Dimocarpus longan* Lour. Front Plant Sci, 6: 1119.

Liu, J., Cheng, X., Liu, D., Xu, W., Wise, R., Shen, Q., 2014. The miR9863 family regulates distinct *Mla* Alleles in barley to attenuate NLR receptor-triggered disease resistance and cell-death signaling. PLoS Genet, 10, e1004755.

Liu, S., Ni, Y., He, Q., Wang, J., Chen, Y., Lu, C., 2017b. Genome-wide identification of microRNAs that respond to drought stress in seedlings of tertiary relict *Ammopiptanthus mongolicus*. Hortic Plant J, 3: 209–218.

Liu, Y., Ke, L., Wu, G., Xu, Y., Wu, X., Xia, R., Deng, X., Xu, Q., 2017a. miR3954 is a trigger of phasiRNAs that affects flowering time in citrus. Plant J, 92: 263–275.

Mano, S., Nakamura, T., Kondo, M., Miwa, T., Nishikawa, S.I., Mimura, T., Nagatani, A., Nishimura, M., 2014. The plant organelles database 3 (PODB3) update 2014: integrating electron micrographs and new options for plant organelle research. Plant Cell Physiol, 55: e1.

Marin, E., Jouannet, V., Herz, A., Lokerse, A.S., Weijers, D., Vaucheret, H., Nussaume, L., Crespi, M.D., Maizel, A., 2010. miR390, *Arabidopsis TAS3* tasiRNAs, and their *auxin response factor* targets define an autoregulatory network quantitatively regulating lateral root growth. Plant Cell, 22: 1104–1117.

Montgomery, T.A., Howell, M.D., Cuperus, J.T., Li, D., Hansen, J.E., Alexander, A.L., Chapman, E.J., Fahlgren, N., Allen, E., Carrington, J.C., 2008. Specificity of ARGONAUTE7-miR390 interaction and dual functionality in *TAS3* trans-acting siRNA formation. Cell, 133: 128–141.

Robinson, J.T., Thorvaldsdóttir, H., Winckler, W., Guttman, M., Lander, E.S., Getz, G., Mesirov, J.P., 2011. Integrative genomics viewer. Nat Biotechnol, 29: 24–26.

Shuai, P., Su, Y., Liang, D., Zhang, Z., Xia, X., Yin, W., 2016. Identification of phasiRNAs and their drought-responsiveness in *Populus trichocarpa*. FEBS Lett, 590: 3616–3627.

Shulaev, V., Sargent, D.J., Crowhurst, R.N., Mockler, T.C., Folkerts, O., Delcher, A.L., Jaiswal, P., Mockaitis, K., Liston, A., Mane, S.P., Burns, P., 2011. The genome of woodland strawberry (*Fragaria vesca*). Nat Genet, 43: 109–116.

Si-Ammour, A., Windels, D., Arn-Bouldoires, E., Kutter, C., Ailhas, J., Meins, F., Vazquez, F., 2011. miR393 and secondary siRNAs regulate expression of the *TIR1/AFB2* auxin receptor clade and auxin-related development of *Arabidopsis* leaves. Plant Physiol, 157: 683–691.

Sosa-Valencia, G., Palomar, M., Covarrubias, A.A., Reyes, J.L., 2017. The legume miR1514a modulates a NAC transcription factor transcript to trigger phasiRNA formation in response to drought. J Exp Bot, 68: 2013–2026.

Šurbanovski, N., Brilli, M., Moser, M., Si-Ammour, A., 2016. A highly specific microRNA-mediated mechanism silences LTR retrotransposons of strawberry. Plant J, 85: 70–82.

Voinnet, O., 2009. Origin, biogenesis, and activity of plant Micrornas. Cell, 136: 669–687.

Wang, K., Su, X., Cui, X., Du, Y., Zhang, S., Gao, J., 2018. Identification and characterization of microRNA during *Bemisia tabaci* infestations in *Solanum lycopersicum* and *Solanum habrochaites*. Hortic Plant J, 4: 62–72.

Wu, M., Tian, Q., Reed, J.W., 2006. *Arabidopsis* microRNA167 controls patterns of *ARF6* and *ARF8* expression, and regulates both female and male reproduction. Development, 133: 4211–4218.

Xia, R., Chen, C., Ma, W., Pokhrel, S., Huang, K., Xu, J., Patel, P., Meyers, B.C., Liu, Z., Xia, R., Wang, F., Li, J., 2019. 24-nt reproductive phasiRNAs are broadly present in angiosperms. Nat Commun, 10: 627.

Xia, R., Meyers, B.C., Liu, Z., Beers, E.P., Ye, S., Liu, Z., 2013. microRNA superfamilies descended from miR390 and their roles in secondary small interfering rna biogenesis in eudicots. Plant Cell, 25: 1555–1572.

Xia, R., Xu, J., Arikit, S., Meyers, B.C., 2015a. Extensive families of miRNAs and *Phas* loci in *Norway spruce* demonstrate the origins of complex phasiRNA networks in seed plants. Mol Biol Evol, 32: 2905–2918.

Xia, R., Xu, J., Meyers, B.C., 2017. The emergence, evolution, and diversification of the miR390-*TAS3*-*ARF* pathway in land plants. Plant Cell, 29: 1232–1247.

Xia, R., Ye, S., Liu, Z., Meyers, B.C., Liu, Z., 2015b. Novel and recently evolved microRNA clusters regulate expansive *F-box* gene networks through phased small interfering RNAs in wild diploid strawberry. Plant Physiol, 169: 594–610.

Xie, J., Yang, X., Song, Y., Du, Q., Li, Y., Chen, J., Zhang, D., 2017. Adaptive evolution and functional innovation of *Populus*-specific recently evolved microRNAs. New Phytol, 213: 206–219.

Xu, X., Yin, L., Ying, Q., Song, H., Xue, D., Lai, T., Xu, M., Shen, B., Wang, H., Shi, X., 2013. High-throughput sequencing and degradome analysis identify miRNAs and their targets involved in fruit senescence of *Fragaria ananassa*. PLoS ONE, 8: e70959.

Yu, B., Yang, Z., Li, J., Minakhina, S., Yang, M., Padgett, R.W., Steward, R., Chen, X., 2005. Methylation as a crucial step in plant microRNA biogenesis. Science, 307: 932–935.

Zhang, X., Zhao, H., Gao, S., Wang, W., Katiyar-Agarwal, S., Huang, H., Raikhel, N., Jin, H., 2011. *Arabidopsis* Argonaute 2 regulates innate immunity via miRNA393*-mediated silencing of a Golgi-localized snare gene, *MEMB12*. Mol Cell, 42: 356–366.